Available online at www.sciencedirect.com
SCIENCE DIRECT®
Journal of Power Sources 119–121 (2003) 45–49
JOURNAL OF POWER SOURCES
www.elsevier.com/locate/jpowsour

Tin-based composite materials as anode materials for Li-ion batteries

J.-H. Ahn[a,*], G.X. Wang[b], J. Yao[b], H.K. Liu[b], S.X. Dou[b]

[a]*Department of Materials Engineering, Andong National University, 388 Songchun-dong, Andong, 760-749 Gyungbuk, South Korea*
[b]*Institute for Superconducting and Electronic Materials, University of Wollongong, Wollongong, NSW 2522, Australia*

Abstract

Tin, tin oxide and NiSn-based nanocomposites with Al_2O_3 dispersion were prepared by ball milling to see their electrochemical properties as a new anode material for lithium-ion batteries. Electrochemical tests demonstrated that the initial charge–discharge capacities are very high for these materials. However, the capacity faded rapidly after the first cycle due to irreversible reactions. This is thought to be caused by the separation of the active materials from the inert oxide particles. The initial cycling efficiency was markedly improved by subsequent annealing of the ball-milled electrode.

Keywords: Mechanical alloying; Nanocrystalline alloys; Lithium-ion batteries; Tin oxides; Anode materials; Secondary batteries

1. Introduction

In recent years, lithium-ion secondary batteries using a graphite anode have rapidly become important for use in a variety of electronic devices. In spite of their successful commercialization, however, various new anode materials have been investigated to overcome the limited capacity of graphite (372 mAh/g) which is less than one-tenth of that of lithium metal (3860 mAh/g). A worldwide effort has been made to search alternative anode materials to replace graphite as anode materials for lithium-ion batteries. Tin-based oxide materials such as SnO_2, SnO and tin glass showed higher specific capacity as anode active materials than carbonaceous materials [1–5]. However, a large irreversible capacity loss at the first cycle due to a reduction/replacement reaction [6] prevents tin oxide anode materials from having any practical application. It was reported that tin oxides are reduced during the first discharge to form fine particles of tin and inactive phases like Li_2O which slows the growth of tin [5]. Due to the reduction of the SnO, tin oxide anodes need an excess of cathode material to be used for compensation. Furthermore, tin oxide particles with large sizes pulverize rapidly during discharge and charge cycles due to volume mismatch, resulting in a rapid drop in reversible capacity upon cycling. This 'pulverization' is to be thought less extensive in the case of smaller particles because the nanometer sized cavities within powders can absorb the expansion of materials during the formation of lithium compounds. Therefore, it is postulated that nanostructured or amorphous electrodes may reduce the extent of pulverization, and in this manner, the cycle life of the electrode is expected to be improved (e.g. [7,8]).

We think that nanocomposites consisting of active and inactive constituents with lithium can be one approach to solve the problem. Finely dispersed inert particles in an active matrix can not only buffer the volume mismatch of electrode materials during cycling but also induce homogeneous expansion. The homogeneous expansion should prevent cracking of the particles.

In the present work, we have investigated the dispersion effect of thermodynamically stable ceramic particle Al_2O_3 on the electrochemical properties of Sn, SnO_2, Sn and tin-based intermetallic Ni–Sn as anode materials for Li-ion batteries.

2. Experimental procedure

The Al_2O_3 powders were added to tin-based matrix of Sn, SnO or NiSn to see enhanced properties. High purity powders, Sn (99.9% pure), SnO_2 and NiSn were used as starting materials for matrix phases. NiSn alloy was prepared by sintering Ni–Sn powder mixture at 1200 °C in vacuum for 2 h, followed by crushing. The dispersed particle was Al_2O_3 (~20 nm). The matrix and dispersing ceramic powders (30 wt.%) were weighed and mixed in a dry argon-filled glove box. The mixture was then milled for 1–20 h using a

* Corresponding author. Tel.: +82-54-820-5648; fax: +82-54-820-6126.
E-mail address: jhahn@andong.ac.kr (J.-H. Ahn).

0378-7753/03/$ – see front matter © 2003 Elsevier Science B.V. All rights reserved.
doi:10.1016/S0378-7753(03)00122-8

Fritsch planetary ball mill. Both vial and ball (∅ 6.4 mm) were made of stainless steel (SUS 304). The weight ratio of the ball to powder was 20:1. X-ray diffraction of the milled powders was carried out with monochromatized Cu Kα radiation at a scan speed of 2° min^{-1}. To observe the structural changes during charge–discharge tests, the electrodes were detached from the cell and coated by Kapton tape to protect the lithiated compound prior to XRD measurement. The microstructure and crystal size were examined both by scanning and transmission electron microscopy.

The electrochemical performance of electrodes was evaluated by following the lithium intercalation process in a cell using a lithium metal counter electrode, i.e. by monitoring the potential of the tin-containing alloy electrode during intercalation and de-intercalation. For the electrochemical performance test, the ball-milled powders were sieved (325 mesh, 38 μm). Nanocomposite electrodes were prepared by coating slurries (active materials (85 wt.%), carbon black (10%) and polyvinylidene fluoride (5%) dissolved in *n*-methyl pyrrolidinone) on a Cu foil substrate. After coating, the electrodes were dried for 24 h at 100 °C and cold-pressed. Coin-type test cells were assembled in an argon-filled glove box using a Celgard 2400 as a separator, 1 M LiPF6, ethylene carbonate (EC)/diethyl carbonate (DEC) (1:1 volume ratio, Merck) as an electrolyte. Li foil (Aldrich, 99.9%) were used as counter and reference electrodes. The cells were tested with constant current and charged and discharged between 0.005 and 2.5 V. The current was typically 30 mA/g, and the current densities were about 0.25 mA/cm^2. For cyclic voltametric measurement, the cell was cycled at a scanning rate of 0.2 mV/s.

3. Results and discussion

Fig. 1 shows the XRD pattern of the powder mixture of Sn-30% Al_2O_3, SnO_2-30% Al_2O_3 and NiSn-30% Al_2O_3 before and after ball milling. No new phase was formed by high-energy ball milling for 20 h. The crystalline peaks of the dispersed ceramic phase are not detected because of its very fine particle size (∼20 nm), although their volume fraction is not low (30%). After milling, diffraction peaks of matrix phase broadened, indicating the reduction of the crystalline size as well as partial amorphization of the matrix phases. In the case of NiSn composition, both NiSn and Ni_3Sn_4 formed by ball milling. Subsequent annealing of ball-milled metastable NiSn composition at 600 °C resulted in the formation of stable NiSn phase with crystalline size of ∼2 μm. TEM examination shows that the matrix phase of the ball-milled powder has an average crystal size of <20 nm with partly amorphized phases.

Fig. 2 illustrates charge–discharge curves of several ball-milled composite electrodes with Al_2O_3 dispersoids. The first charge (Li-insertion) capacities of the Sn-Al_2O_3 electrode was as high as 980 mAh/g, while that of SnO_2-Al_2O_3 electrode was 600 mAh/g. In the case of NiSn matrix, the

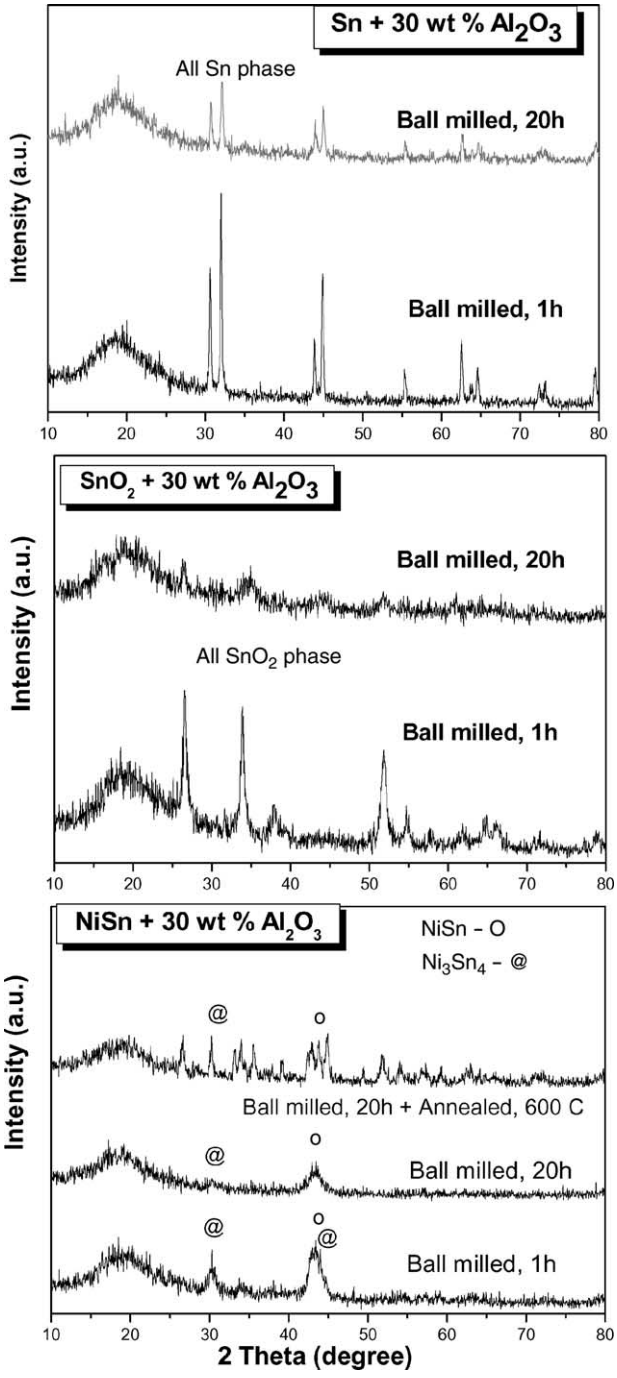

Fig. 1. The XRD pattern of the powder mixture of Sn-30% Al_2O_3, SnO_2-30% Al_2O_3 and NiSn-30% Al_2O_3.

first charge capacity of ball-milled nanocrystalline electrode was 429 mAh/g. This value decreased to 250 mAh/g when using annealed microcrystalline electrode. The initial cycling efficiency was very low for ball-milled powders: only 20% for Sn-Al_2O_3 electrode. On the other hand, an initial cycling efficiency of ∼90% was observed for annealed NiSn microcrystalline electrode, although the capacity value was low from the annealing process. Fig. 3

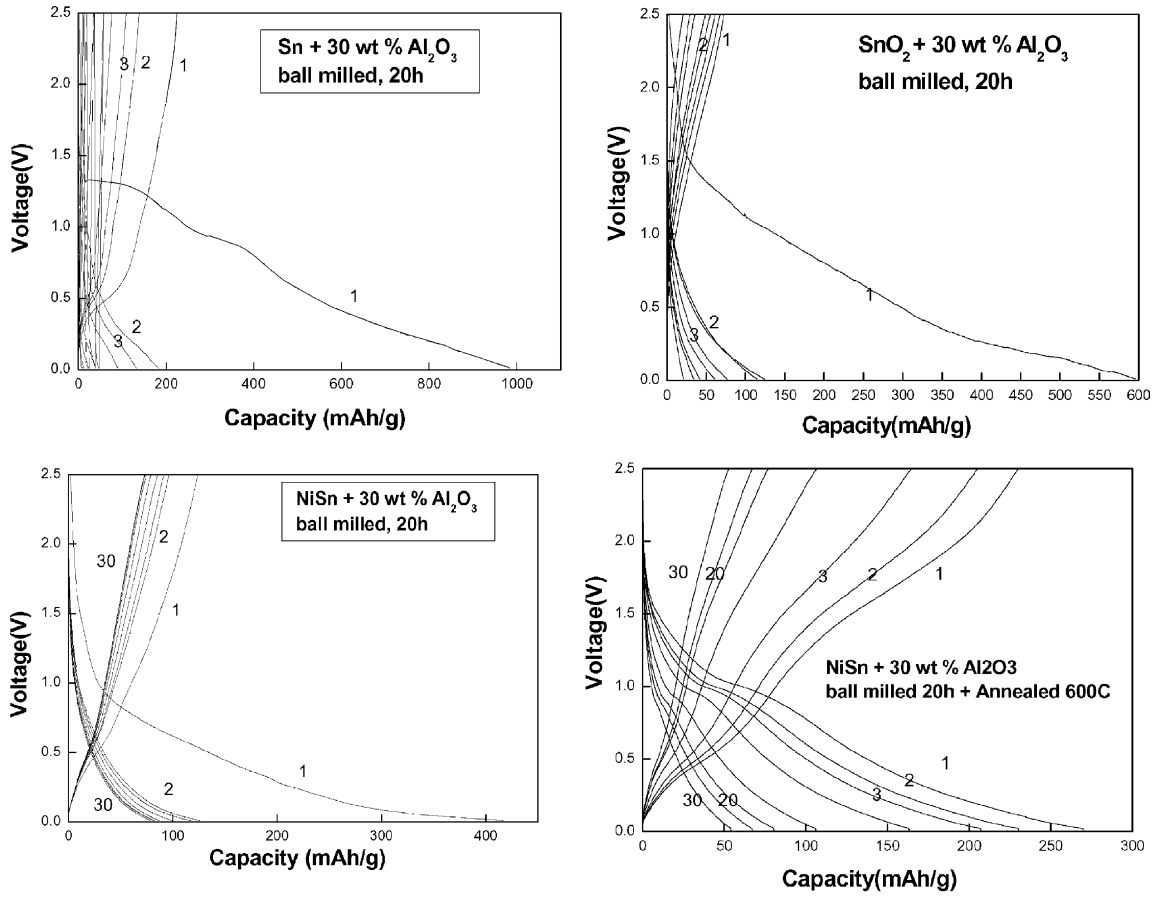

Fig. 2. Charge–discharge curves of ball-milled composite electrodes with Al_2O_3 dispersion.

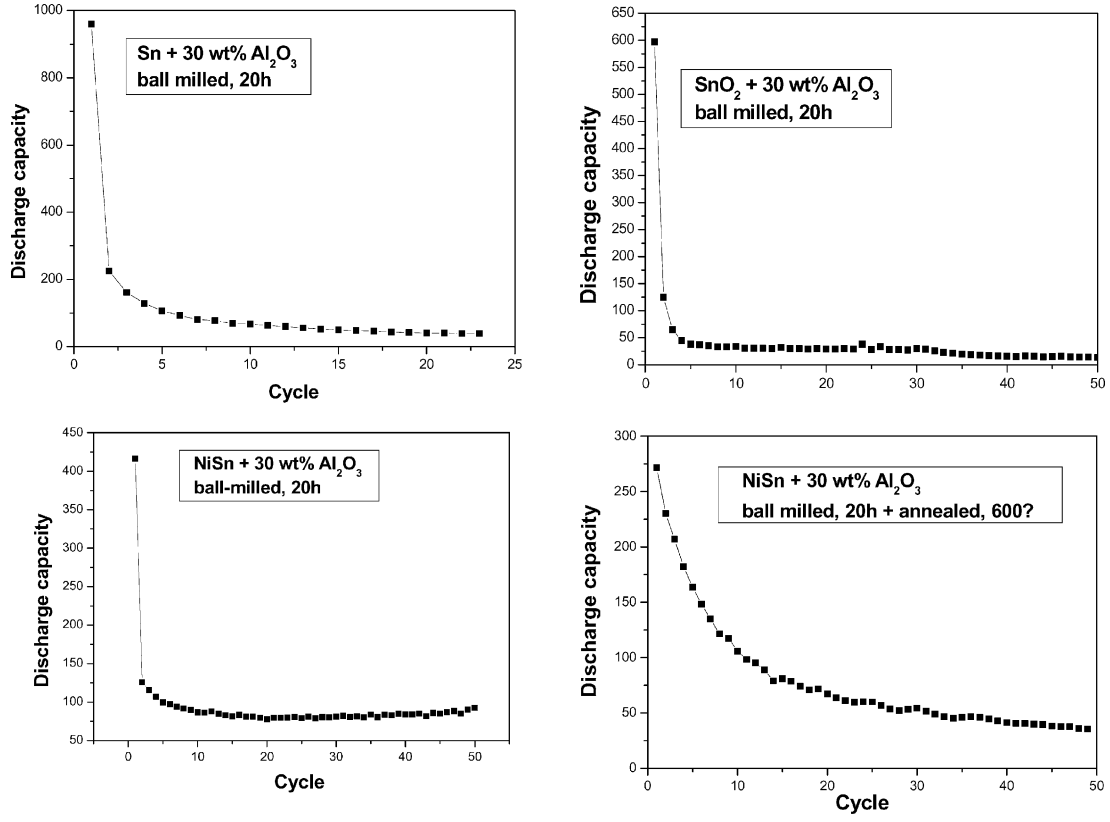

Fig. 3. Change in charge capacities on cycling for the nanocomposite electrodes.

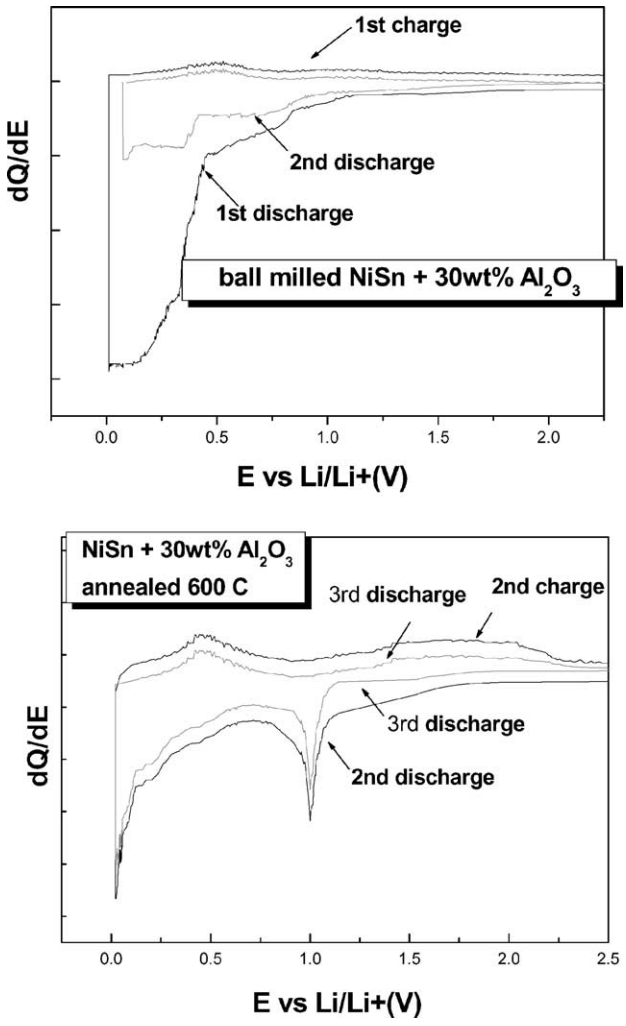

Fig. 4. Differential capacity vs. voltage curves for NiSn-Al_2O_3 electrodes.

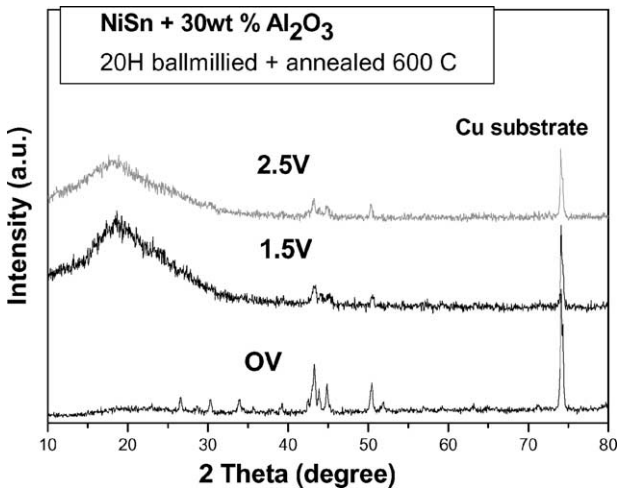

Fig. 5. Change in XRD peak patterns after lithiation for the NiSn-Al_2O_3 electrodes.

illustrates the discharge capacity versus cycle curves. The capacity of the electrode with nanocrystalline matrix phase dropped rapidly, while a slow decline of capacity on cycling for the annealed microcrystalline NiSn electrode was observed. In order to see the reaction during charge/discharge, differential capacity versus voltage profiles were examined for the NiSn-based electrode (Fig. 4). For the ball-milled NiSn-Al_2O_3 electrode, abnormally deviated lines of the first discharge curves can be seen, showing a considerable electrolyte decomposition during the first cycle. In contrast, the annealed microcrystalline NiSn-Al_2O_3 electrode exhibits a moderate reaction after the second cycle showing that both the oxidation and reduction peaks retained their position relatively well.

The observed high capacity of the ball-milled nanocomposites indicates that the charges consumed in the first charging process of the ball-milled electrode exceeds the expected maximum theoretical capacities. The maximum lithium insertion theoretically predictable should be 724 mAh/g provided that the Li_4Sn_{22} phase forms. This excess capacity for ball-milled nanocrystalline powder is supposed to be caused by side reaction involving the decomposition of the electrolyte which induces the formation of a passivating film on the electrode surfaces. A supplementary decomposition of the electrolyte is possible for the ball-milled electrode due to the extended solubility of nanocrystalline materials. Also, Li ions might be more abundantly inserted in the ball-milled electrode than in conventional alloys because nanocrystalline powders contain a high volume fraction of grain boundaries having loose atomic packing structures.

The observed poor cyclability of the oxide dispersed electrode is thought to be caused by the separation of the active materials (tin-based materials) from the inert oxide particles. It is presumed that non-conductive inert particles are detached from the composite electrode by the swelling of tin-based matrix phase during cycling. Another possible cause might be some irreversible reactions of tin or tin oxide occurs due to their extremely fine crystal size. It is well-known that nanocrystalline materials sometimes exhibit unusual solubility and reactivity which cannot be predicted by the equilibrium phase diagram. In the present work, we could not identify the details of such reactions. However, broadening of X-ray diffraction peaks after lithiation confirmed that the tin-based nanocomposite electrolytes amorphized extensively or pulverized into fine grains (Fig. 5).

4. Conclusions

We have synthesized various tin-based nanocomposite anodes with Al_2O_3 dispersion, using high-energy ball milling. The first charge (Li-insertion) capacities are very high for these composite electrodes. Contrary to our expectation, the nanosize oxide dispersion did not improve cycle

properties of tin-based anodes. The 'pulverization', which is to be thought less extensive in the case of smaller particles, was not observed, although subsequently annealed microcrystalline electrode exhibited better cycle properties and better coulomb efficiency than nanocrystalline electrodes. This is thought to be caused by the separation of the active materials from the inert oxide particles, abnormally extended solubility or reactivity of nanocrystalline electrodes, leading to irreversible reactions during cycling.

Acknowledgements

The authors are grateful for the financial support of the Korean Center for Advanced Materials Center and Australian Research Council.

References

[1] J. Wolfenstine, J. Sakamoto, C.K. Huang, J. Power Sources 75 (1998) 181.
[2] T. Brousse, R. Retpix, U. Herterich, D.M. Sleich, J. Electrochem. Soc. 145 (1998) 1.
[3] W. Liu, X. Huang, Z. Wang, H. Li, L. Chen, J. Electrochem. Soc. 145 (1998) 59.
[4] G.R. Goward, F. Leroux, W.P. Power, G. Ouvrard, W. Domowski, T. Enami, L.F. Nazar, Electrochem. Solid-State. Lett. 2 (1999) 367.
[5] I.A. Courtney, W.R. McKinnon, J.R. Dahn, J. Electrochem. Soc. 146 (1999) 59.
[6] I.A. Courtney, J.R. Dahn, J. Electrochem. Soc. 144 (1997) 2045.
[7] J. Yang, M. Wachtler, M. Winter, J.O. Besenhard, Electrochem. Solid-State Lett. 2 (1999) 161.
[8] O. Mao, R.L. Turner, I.A. Courtney, B.D. Frederickson, M.I. Buckett, L.J. Krausse, J.R. Dahn, Electrochem. Solid-State Lett. 2 (1999) 547.